ChemComm

COMMUNICATION

View Article Online
View Journal

Metallamacrocycle-modified gold nanoparticles: a new pathway for surface functionalization†‡

Cite this: DOI: 10.1039/c3cc47722c

Received 9th October 2013,
Accepted 29th October 2013

DOI: 10.1039/c3cc47722c

www.rsc.org/chemcomm

Hai-Xia Liu,§ Xin He§ and Liang Zhao*

We report herein the designed synthesis of four silver(I)- or gold(I)-bridged flexible metalla-macrocycles (MMCs) and their distinct performance in the surface modification of gold nanoparticles (AuNPs). The resulting gold(I)-MMCs-modified AuNPs were found to be resistant to pH variation and capable of binding with metal ions.

Surface chemical modification of gold nanoparticles (AuNPs), one of the most popular and extensively used metal nano-materials, is of fundamental importance in preventing aggregation, realizing hierarchical assembly and affecting properties of AuNPs.[1] In this regard, organic macrocyclic ligands, such as cyclodextrins,[2] cucurbiturils[3] and calixarenes,[4] have recently attracted intense interests since the endowment of abundant molecular recognition properties of macrocyclic host molecules to AuNPs can largely expand potential applications of AuNPs as nanosensors,[5] and drug delivery vehicles[6] *etc.* During the past two decades, metalla-macrocycles (MMCs)[7] constructed by metal–ligand coordination self-assembly have emerged as a new type of macrocyclic compounds, which can serve as precursors of functional materials,[8] reagents for molecular recognition,[9] or cavity controlled catalysts.[10] Despite such versatile functionalities, however, MMCs have been scarcely employed in the functionalization of AuNPs by surface modification possibly due to their moderate stability and rigid skeletons.

Recent single-crystal X-ray analysis of some reported gold–thiolate nanoclusters[11] has shown that while the cores of these nanoclusters are composed of Au atoms in high symmetry, their surface layers usually consist of a number of outermost Au atoms bridged by thiolate ligands to form a series of $Au_m(SR)_n$ flexible semi-ring structures.[12] These peripheral Au atoms ultimately bind with the nanocluster core *via* significant aurophilic interaction.[13] Inspired by this $[Au_x]_{central}$–$[Au_m(SR)_n]_{peripheral}$ core–shell structural model, we envision that gold(I)-contained flexible MMCs may be capable of modifying the surface of AuNPs by aurophilic interactions.

To achieve stable gold-bridged MMCs, we selected N-heterocyclic carbenes (NHCs) as organic donor species for binding to gold(I) atoms in view of the high bond dissociation energy of Au–$C_{(NHC)}$ (calculated D_e = 80 kcal mol^{-1}),[14] which is >20 kcal mol^{-1} larger than the Au–S bond in common thiolate-protected AuNPs.[15] The pyridine oligomer species (Scheme 1) were introduced as not only a linking unit but also a stabilizing one to fix the conformation of the flexible polypyridine arm by use of a possible chelation based on carbene and pyridyl nitrogen coordination sites. Two bridging metal atoms (Ag(I) and Au(I)) were adopted to probe the influence of different metallophilic interactions (Ag–Au and Au–Au, respectively) in the surface modification of AuNPs.

As shown in Scheme 1, two diimidazolium salts $(H_2\text{-}\mathbf{1})(PF_6)_2$ and $(H_2\text{-}\mathbf{2})(PF_6)_2$ were first prepared by the reaction of imidazole with dibromo-substituted pyridine trimer or pentamer followed by methylation and anion exchange with NH_4PF_6. Treatment of $(H_2\text{-}\mathbf{1})(PF_6)_2$ and $(H_2\text{-}\mathbf{2})(PF_6)_2$ by silver oxide in dichloromethane–acetonitrile yielded two silver-bridged organometallic macrocycles **MMC-1** and **MMC-2**. The silver atoms in these two

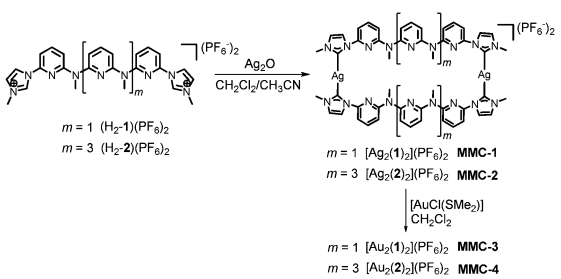

Scheme 1 Synthetic procedures for **MMC-1–4**.

Department of Chemistry, Key Laboratory of Bioorganic Phosphorus Chemistry & Chemical Biology (MOE), Tsinghua University, Beijing 100084, China. E-mail: zhaolchem@mail.tsinghua.edu.cn

† This work is dedicated to Professor James Trotter in celebration of his 80th birthday.

‡ Electronic supplementary information (ESI) available: Synthetic procedures and characterization data for **MMC-1–4**. CCDC 964573 and 964574. For ESI and crystallographic data in CIF or other electronic format see DOI: 10.1039/c3cc47722c

§ These authors contributed equally.

complexes can be substituted by gold(I) atoms to produce two gold(I)-bridged macrocycles **MMC-3** and **MMC-4**.

Formation of flexible macrocyclic **MMC-1–4** was confirmed by NMR, mass spectrometry and single-crystal X-ray crystallography. A simple one set of NMR signals corresponding to the protons at asymmetrical positions in the molecular structures of **MMC-1–4** suggests a highly flexible conformation of **MMC-1–4** in solution at ambient temperature. After transmetalation from **MMC-1–2** to **MMC-3–4**, the proton signals corresponding to the imidazolium rings undergo a downfield shift (0.1–0.2 ppm), implying a stronger electron-withdrawing ability of the gold(I) atom. ESI-MS spectra of **MMC-1–4** clearly showed the peaks corresponding to the M_2L_2 stoichiometric complexes.

An X-ray diffraction study with crystals of **MMC-1**·$CH_3OCH_2CH_2OCH_3$ confirmed the 2 : 2 metal : ligand composition and macrocyclic structure of **MMC-1** (Fig. 1a). The metric parameters found in this crystal structure [Ag–$C_{carbene}$ = 2.049(17)–2.139(14) Å; ∠ $C_{carbene}$–Ag–$C_{carbene}$ = 171.6(7)–177.1(7)°] fall in the range previously described for linear silver dicarbene complexes.[16] The close contacts (~2.8 Å) between two silver(I) atoms (Ag1 and Ag2) and two pyridyl nitrogen atoms (N7 and N16) substantiate our design that the coordination of adjacent pyridyl nitrogen atoms indeed influences the conformational fixation of the resulting flexible MMCs. Crystallization of **MMC-4** is more challenging due to the existence of two long pyridine pentamers. We supposed that intramolecular hydrogen bonding within the pyridine pentamer species may be helpful in rigidifying the conformation of **MMC-4**. Upon the addition of triflate acid into an acetonitrile solution of **MMC-4** in the crystallization process, pale-yellow crystals of a protonated **MMC-4** complex $[H_2Au_2(\mathbf{2})_2(H_2O)_2](CF_3SO_3)_4{\cdot}H_2O$ were finally acquired. X-Ray crystallographic analysis revealed that each gold(I) ion is linearly coordinated by two NHC donors with Au–C distances in the range of 2.012–2.033 Å (Fig. 1), consistent with values in other Au–C_{NHC} complexes.[17] The whole structure can be divided into a helical unit and a pincer-like Py–NHC–Au–NHC–Py (Py = pyridine) species. In the helical unit, two protonated pyridine rings (N9 and N18 in Fig. 1b) constitute hydrogen-bonding with their adjacent pyridine rings. Noticeably, two NHC moieties around the same gold(I) center are almost coplanar with each other, consequently leaving the gold(I) center laterally reachable.

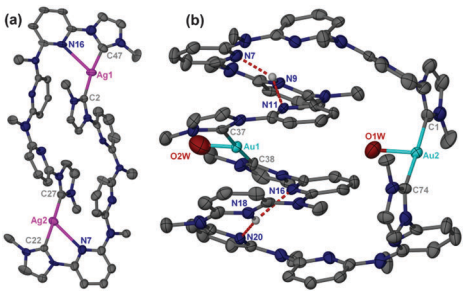

Fig. 1 Crystal structures of (a) **MMC-1**·$CH_3OCH_2CH_2OCH_3$ and (b) $[H_2Au_2(\mathbf{2})_2(H_2O)_2](CF_3SO_3)_4{\cdot}H_2O$ (a protonated **MMC-4**). Uncoordinated water and $CH_3OCH_2CH_2OCH_3$ molecules, PF_6^- and $CF_3SO_3^-$ anions, and hydrogen atoms are omitted for clarity. Color scheme for atoms: Ag, purple; Au, cyan; C, black; N, blue; O, red.

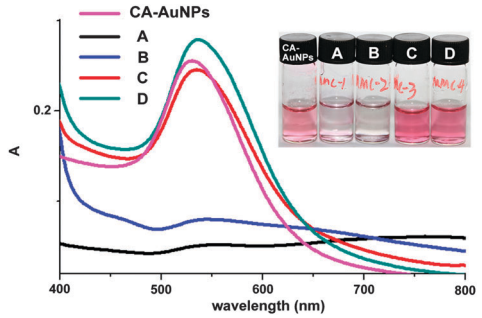

Fig. 2 UV-vis spectra of **CA-AuNPs** and MMC-modified AuNPs (**A–D**) in DMF–H_2O (v/v = 9 : 1) solution. (inset) Photographs of solution samples of **CA-AuNPs** and **A–D**.

Employment of **MMC-1–4** to modify the surface of AuNPs was implemented by a ligand-exchange reaction. The citrate-protected AuNPs (**CA-AuNPs**) were first synthesized by a literature method.[18] Addition of the *N*,*N*-dimethylformamide (DMF) solution of **MMC-1–4** into the red aqueous solution of **CA-AuNPs** generated distinct results. Upon addition of the silver(I)-bridged macrocycles **MMC-1** or **-2**, the AuNPs solution samples (abbreviated as **A** and **B**, respectively) became gray within a few minutes. The UV-vis spectra of **A** and **B** (Fig. 2) revealed that the surface plasmon resonance peak of AuNPs at around 530 nm decreased dramatically relative to **CA-AuNPs**, suggesting possible aggregation and precipitation of AuNPs. In contrast, the mixed solution samples of AuNPs and **MMC-3** or **-4** (**C** and **D**, respectively) remained the same red color as **CA-AuNPs**. The surface plasmon resonance peak in **C** and **D** both underwent a slight red shift from 530 (**CA-AuNPs**) to 535 nm.

Transmission electron microscope (TEM) images provided further evidence for the distinct performance of **MMC-1–4** in samples **A–D**. As shown in Fig. 3, the images of freshly prepared **CA-AuNPs** displayed some small aggregates composed of several spherical particles (size: 41.7 ± 8.7 nm). These small aggregates were found to densely assemble into large networks in samples **A** and **B** upon the addition of the silver-bridged macrocycles **MMC-1** and **-2**. This observation is in good agreement with the UV-vis results.

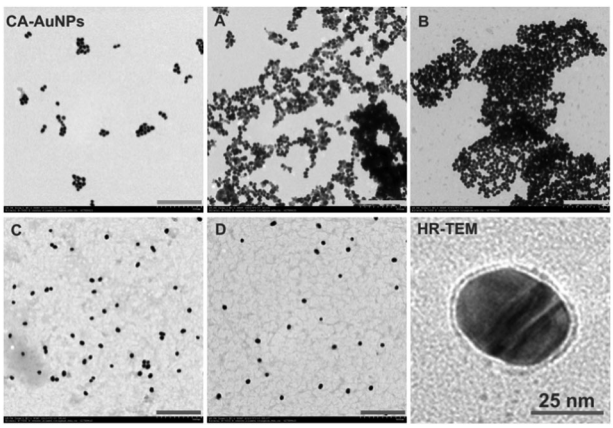

Fig. 3 TEM images of **CA-AuNPs** and MMC-modified AuNPs (**A–D**). Scale bar = 500 nm. The high resolution-TEM image shows a gold nanoparticle in **D** protected by a monolayer.

In contrast, the TEM images of samples **C** and **D** showed that in these two samples the AuNPs were mostly well-dispersed as discrete species. The reason for such good dispersity may be ascribed to the surface decoration by a number of positively charged gold(I)-MMCs, which increase the surface positive charge density of each AuNPs and make them electrostatically repel to each other. Considering the gold(I)-containing molecular structures of **MMC-3** and **-4**, it is possible to obtain direct imaging of the MMCs-based monolayer around the periphery of AuNPs.[19] As shown in Fig. 3, high-resolution TEM revealed that most AuNPs in sample **D** indeed possess a discernible monolayer shell. The thickness of this monolayer is around 0.8 ± 0.1 nm, comparable to the dimension of **MMC-4** measured in its crystal structure.

Samples **A–D** were then purified by centrifugation to remove unbound MMCs and citrate ligands. In the Fourier transform infrared (FT-IR) spectra of the centrifuged samples (Fig. S1–S9 in ESI‡), the typical absorptions at *ca.* 2924 cm^{-1} arising from the C–H stretching of the methyl groups in the pyridine oligomers were observed, indicating the inclusion of the organic NHC species (**1** and **2** in Scheme 1) in these nanoparticle samples.

The different performance of **MMC-1–2** and **MMC-3–4** in the surface modification of AuNPs was then investigated. It is well known that silver(I)–NHC compounds can undergo a Ag-transfer process to synthesize other metal-centered NHC complexes,[20] driven by the formation of insoluble silver salts (such as AgCl in the transmetalation process from **MMC-1–2** to **MMC-3–4**). We hypothesized that a similar transmetalation may take place as well between **MMC-1** or **-2** and the surface gold atoms of **CA-AuNPs.** The formation of silver citrate, an undissolved polymeric precipitate, may drive the occurrence of this reaction, consequently resulting in the cross-linking and aggregation of AuNPs.

In order to clarify the interaction between gold(I) macrocycles **MMC-3–4** and AuNPs, the following characterization and control experiments were carried out. X-Ray photoelectron spectroscopy (XPS) measurement of the centrifuged sample **D** (Fig. S10, ESI‡), which excludes the unbound **MMC-4**, revealed two Au $4f_{7/2}$ peaks with binding energies of 88.22 and 84.52 eV. These values are different from **CA-AuNPs** (87.47 and 83.77 eV) but very close to the values of **MMC-4** (88.44 and 84.97 eV). We speculated this may result from the abundant distribution of **MMC-4** on the surface of AuNPs. Attempts to characterize aurophilic interaction between the surface gold atoms of AuNPs and the gold(I) atoms in **MMC-3** or **-4** by surface-enhanced Raman spectroscopy (SERS) were unsuccessful. Therefore, we tried to perform the following contrast experiments to elucidate the interaction between MMCs and AuNPs. In contrast to the **CA-AuNPs** that produced severe aggregation of AuNPs upon the addition of only a small amount of HBF_4 (pH value is lowered to 2), the **MMC-3** or **-4** modified AuNPs can preserve their coloration and surface plasma resonance peak intensity at pH = 2 (Fig. S11–S13, ESI‡). Such acid resistance arising from the proton binding by free pyridyl nitrogen atoms of **MMC-3** or **-4** indicates that the coordination of pyridyl nitrogen atoms with the surface gold atoms of AuNPs has small contribution in the ligation between MMCs and AuNPs.

The coordination ability of **MMC-3** and **-4** in samples **C** and **D** was further evaluated with $[Cu(CH_3CN)_4](PF_6)$ as a probe (Fig. S14, ESI‡). Mixing a DMF solution of $[Cu(CH_3CN)_4](PF_6)$ with **CA-AuNPs** led to the disappearance of the characteristic red color of well-dispersed AuNPs. This is probably because of the coordination-based cross-linkage between citrates and copper(I) ions. However, adding Cu(I) ions (up to 5 fold relative to MMCs) into the **MMC-3** or **-4** modified AuNPs solution did not change its red color. UV-vis spectra revealed that the surface plasma resonance peak in these two samples kept its intensity but red-shifted 2–3 nm. In addition, the UV-vis absorption peak at around 325 nm due to the $\pi \rightarrow \pi^*$ transition of pyridine oligomer species were located at identical positions with the MMC–$[Cu(CH_3CN)_4](PF_6)$ complexes. This suggests the MMCs in samples **C** and **D** behave like free macrocycles and their coordination with copper(I) ions did not influence the stability of AuNPs. We thus concluded that aurophilic interaction rather than coordination may play a significant role in the binding between **MMC-3–4** and AuNPs.

In summary, we have described the designed synthesis of four MMCs by a side-chain-assisted approach. The silver(I)-bridged MMCs can undergo transmetalation to form a network aggregation of AuNPs, while the gold(I)-bridged ones were found to anchor onto the surface of AuNPs. The coordinative pyridyl nitrogen atoms of MMCs in these Au(I)-MMC-modified AuNPs can further bind with protons and metal ions, indicating their future application in molecular recognition and hierarchical assembly. The herein demonstrated use of MMCs to decorate the surface of metal nanoparticles is an important step forward in efforts to provide a new stabilizing effect as well as establish a promising method to access structurally and functionally diverse modified nanoparticles.

Financial support by the NSFC (21002057, 91127006, 21132005, 21121004), MOST (2013CB834501, 2011CB932501), MOE (NCET-12-0296) and Tsinghua University (2011Z02155) is gratefully acknowledged. We are grateful to Prof. Zhong-Qun Tian and Mr. Chao-Yu Li at Xiamen University for helpful discussions.

Notes and references

1 A. C. Templeton, W. P. Wuelfing and R. W. Murray, *Acc. Chem. Res.*, 2000, **33**, 27; J. C. Love, L. A. Estroff, J. K. Kriebel, R. G. Nuzzo and G. M. Whitesides, *Chem. Rev.*, 2005, **105**, 1103.
2 J. Liu, S. Mendoza, E. Román, M. J. Lynn, R. L. Xu and A. E. Kaifer, *J. Am. Chem. Soc.*, 1999, **121**, 4304.
3 T.-C. Lee and O. A. Scherman, *Chem. Commun.*, 2010, **46**, 2438.
4 T. R. Tshikhudo, D. Demuru, Z. Wang, M. Brust, A. Secchi, A. Arduini and A. Pochini, *Angew. Chem., Int. Ed.*, 2005, **44**, 2913.
5 R. de la Rica and A. H. Velders, *Small*, 2011, **7**, 66.
6 C. Kim, S. S. Agasti, Z. J. Zhu, L. Isaacs and V. M. Rotello, *Nat. Chem.*, 2010, **2**, 962.
7 For some recent reviews, see: T. R. Cook, Y.-R. Zheng and P. J. Stang, *Chem. Rev.*, 2013, **113**, 734; M. J. Smulders, I. A. Riddell, C. Browne and J. R. Nitschke, *Chem. Soc. Rev.*, 2013, **42**, 1728; Y. Inokuma, M. Kawano and M. Fujita, *Nat. Chem.*, 2011, **3**, 349.
8 J.-S. Chen, G.-J. Zhao, T. R. Cook, K.-L. Han and P. J. Stang, *J. Am. Chem. Soc.*, 2013, **135**, 6694.
9 S. Freye, R. Michel, D. Stalke, M. Pawliczek, H. Frauendorf and G. H. Clever, *J. Am. Chem. Soc.*, 2013, **135**, 8476.
10 T. Murase, Y. Nishijima and M. Fujita, *J. Am. Chem. Soc.*, 2012, **134**, 162.

11 P. D. Jadzinsky, G. Calero, C. J. Ackerson, D. A. Bushnell and R. D. Kornberg, *Science*, 2007, **318**, 430.
12 H. Häkkinen, *Nat. Chem.*, 2012, **4**, 443; R. Jin, Y. Zhu and H. Qian, *Chem.–Eur. J.*, 2011, **17**, 658.
13 H. Schmidbaur and A. Schier, *Chem. Soc. Rev.*, 2008, **37**, 1931.
14 C. Boehme and G. Frenking, *Organometallics*, 1998, **17**, 5801.
15 A. V. Zhukhovitskiy, M. G. Mavros, T. Van Voorhis and J. A. Johnson, *J. Am. Chem. Soc.*, 2013, **135**, 7418.
16 J. C. Y. Lin, R. T. W. Huang, C. S. Lee, A. Bhattacharyya, W. S. Hwang and I. J. B. Lin, *Chem. Rev.*, 2009, **109**, 3561.
17 A. Rit, T. Pape and F. E. Hahn, *J. Am. Chem. Soc.*, 2010, **132**, 4572.
18 G. Frens, *Nature, Phys. Sci.*, 1973, **241**, 20.
19 K. Zhang, Y. Zha, B. Peng, Y. Chen and G. N. Tew, *J. Am. Chem. Soc.*, 2013, **135**, 15994.
20 H. M. J. Wang and I. J. B. Lin, *Organometallics*, 1998, **17**, 972.

